

Fabrication and determination of performance parameters of a pyrene-based organic thin-film transistor

A. Amell, D. Martí, and J. C. Morales

Supervisor: Dr. J. Puigdollers*

Escola Tècnica Superior de Telecomunicació de Barcelona

Universitat Politècnica de Catalunya

(Dated: May 21, 2016)

Organic semiconductors broaden the applications of thin-film transistors, as a flexible substrate can be used. Hence, many organic semiconductors are being studied in the search for high-mobility organic semiconductors. Nevertheless, pyrene-based organic semiconductors have not been studied exhaustively. In this project we aim to reproduce and determine the key performance parameters of a pyrene-based OTFT presented in [1].

Keywords: pyrene, organic semiconductors, thin films, field-effect transistors

I. INTRODUCTION

A thin-film transistor (TFT) is a three-terminal device, in which a voltage applied to a gate electrode controls current flow between a source and drain electrode under an imposed bias. The basic design and function of an organic TFT (OTFT) is analogous to the inorganic TFTs.

The active semiconductor layer of an ordinary inorganic device consists of lightly doped Si, or combinations of Group III-IV elements, such as GaAs. The voltage applied to the gate causes an accumulation of minority charge carriers at the dielectric interface, i.e. an inversion layer. In an organic transistor, the active layer is made up of a thin film of highly conjugated small molecules or polymers. A remarkable difference to inorganic materials is that organics pass current by majority carriers, and an inversion layer does not exist: this phenomenon is related to the nature of charge transport.

OTFTs are particularly interesting as their fabrication processes are much less complex than the conventional inorganic fabrication technology, which requires high-temperature and high-vacuum deposition processes and sophisticated patterning methods. Moreover, the intrinsic mechanical flexibility of organic

materials makes them suitable for flexible substrates for lightweight and foldable products, such as flexible circuits and displays, smart cards and textiles, and even radio frequency identification (RFID), which would serve as smart tags for inventory control [2].

The active layer component of OTFTs limits the current organic technologies. The organics presenting the best electronic characteristics to date are insoluble and therefore difficult to process, such as pentacene [3]. Consequently, much effort has been devoted to developing organic semiconductors which not only meet the performance criteria but also are easy to process with long-term stability. In addition, there is an interest in designing and discovering organic semiconductors which are cost-effective to supply the growing need of substituting silicon [4].

Many researchers have designed aromatic compounds as organic semiconductors for OTFTs. However, pyrene-based (an aromatic compound consisting of four fused benzene rings) organic semiconductors with high performance parameters have not been studied exhaustively. The properties provided by the highly ordered crystalline structure and the fused-ring aromatic structure suggest that pyrene-based semiconductors will give good performance parameters, in contrast to pyrene derivatives [5, 6].

In this paper, we report the fabrication of an OTFT, using a pyrene-based p-type semiconductor, 1,6-bis(5'-octyl-2,2'-bithiophen-5-yl)pyrene (BOBTP). The field-effect mobility

* To whom correspondence should be addressed.
E-mail: joaquim.puigdollers@upc.edu

(μ), threshold voltage (V_t), on-off current ratio ($I_{\text{on}}/I_{\text{off}}$) and subthreshold slope (SS) were calculated to determine the performance of our OTFT.

II. PERFORMANCE PARAMETERS

When the drain current of an OTFT is in the saturation regime, i.e. $|V_{\text{ds}}| \geq |V_{\text{gs}} - V_t|$, it depends quadratically on the gate voltage,

$$I_d = \frac{W}{L} \frac{\mu C_i}{2} (V_{\text{gs}} - V_t)^2 \quad (1)$$

where W/L is the aspect ratio of the transistor, μ is the field-effect mobility and C_i is the geometric capacitance of the dielectric layer, given by

$$C_i = \epsilon_r \epsilon_0 / t_{\text{ox}} \quad (2)$$

where ϵ_r is the relative permittivity of the dielectric layer, ϵ_0 is the vacuum permittivity, and t_{ox} is the width of the dielectric layer. The mobility in the saturation regime [7], can be calculated as

$$\mu = \frac{2L}{WC_i} \left(\frac{\partial \sqrt{I_d}}{\partial V_{\text{gs}}} \right)^2 \quad (3)$$

The on-off current ratio $I_{\text{on}}/I_{\text{off}}$ is the figure of merit that characterizes the difference between the on and off state current. The subthreshold slope SS is a current-voltage characteristic related to how rapid a transistor can switch between the on and off state. The lower the subthreshold slope is, the better is the performance. Both parameters can be obtained from a logarithmic plot of the drain current versus gate voltage with drain, source, and bulk voltages fixed. The calculated performance parameters are summarized in Table I.

III. DEVICE DESIGN AND FABRICATION

The structure of the fabricated device is similar to one of the typical MOSFET structures, the top-contact bottom-gate. However, the construction used is slightly different, and it is illustrated in Fig. 1.

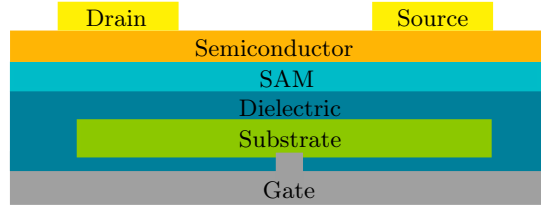


Figure 1. BOBTP OTFT construction type. The gate and the substrate are connected with an embedded drop of silver.

For the device fabrication the following materials were used: gold for the drain and source contacts, a thin layer of BOBTP as the organic semiconductor, a 110 nm thick silicon dioxide (SiO_2) layer for the dielectric with a self-assembled monolayer (SAM) of polystyrene, and an aluminum foil for the gate contact. The dielectric layer was synthesized in the clean room facilities at UPC: the silicon substrate was put in contact with an oxygenated atmosphere at about 1000 °C, and an oxide layer grew around the substrate, consequently obtaining the dielectric and substrate assembly.

To obtain the device, magnetic shadow masks were used to define the transistor areas with precision during the deposition processes, by covering the target surface. The deposition process was carried out by thermal evaporation. In order to do that, first of all we put in a vacuum chamber designed to perform deposition processes the BOBTP material with an already made assembly of substrate, gate and dielectric (SAM included), supplied by the lab. We left the vacuum chamber working for 24 h until a pressure of 1×10^{-7} mPa was reached. Next, we thermally evaporated the BOBTP at around 225 °C with an approximate deposition rate of 0.3 \AA s^{-1} , until the thickness of the semiconductor layer was 50 nm.

Once the deposition of BOBTP was over, the fabricated piece was put into another vacuum chamber, used specifically to evaporate gold to make the drain and source contacts. A gold filament of 5 mm was heated up and evaporated onto the shadow masks defining the contacts on the assembled transistor piece. We have to say that this second procedure did not work out the first time as it damaged the transistor, probably because we heated too

Table I. Key parameters for our BOBTP OTFT for different dates of measurement, and from [1].

Compound	Measurement date	Dielectric surface	μ (cm ²)	V_t (V)	I_{on}/I_{off} (A A ⁻¹)	SS (V dec ⁻¹)
BOBTP ^a	04/20/2016	PS/SiO ₂	0.066	-25.97	$\sim 2.0 \times 10^5$	3.75
BOBTP	04/29/2016	PS/SiO ₂	0.187	-5.85	$\sim 1.6 \times 10^5$	2.45
BOBTP ^b	—	OTS/SiO ₂	2.1	-17.5	$\sim 7.6 \times 10^6$	0.94

^a Parameters determined for $V_{ds} = -30$ V, $W/L = 2$ mm/80 μ m, and $C_i = 31.4$ nF cm⁻² at room temperature.

^b From [1]: $W/L = 1000$ μ m/110 μ m, $C_i = 11.8$ nF cm⁻², BOBTP layer thickness of 110 nm, and $V_{ds} = -40$ V.

much the gold vacuum chamber. Therefore, we had to perform another fabrication of the OTFT.

IV. DISCUSSION

For the purpose of observing the stability of the OTFT over time, we measured it right after the fabrication and once again one week after. We generated three characteristic curves of the transistor. In the output characteristic from the first day (Fig. 2), it can be seen that the transistor presents a good behavior, providing a higher drain current than the one obtained with other organic materials. However, it needs a very high drain voltage to start conducting. This may be due to the crowding effect, a phenomenon in which the carriers are prevented of being picked up at the vicinity of the contacts.

Analyzing the saturation characteristic (Fig. 3a), it can be seen that it is linear in the saturation regime. Observing the graph, it is easy to notice that the threshold voltage is quite large, probably due to the crowding effect previously mentioned.

The same characteristic curves were obtained one week after. The output was similar to the one obtained the first day of measurements. On the other hand, the saturation curve presents a very significant change, as it can be seen in Fig. 3c. It can be appreciated that the current slope is much higher, causing a great improvement in the mobility. The threshold voltage has also increased from -25.97 V to -5.86 V. The evolution of the transfer curve (Figs. 3b and 3d) has also a significant change: the current has a higher output value and the transistor starts to conduct much before after one week of being fabricated.

This shift can be due to the oxygen exposure of the cell, that leads to the formation of acceptors states in the band gap, reducing the impact of the crowding effect [8].

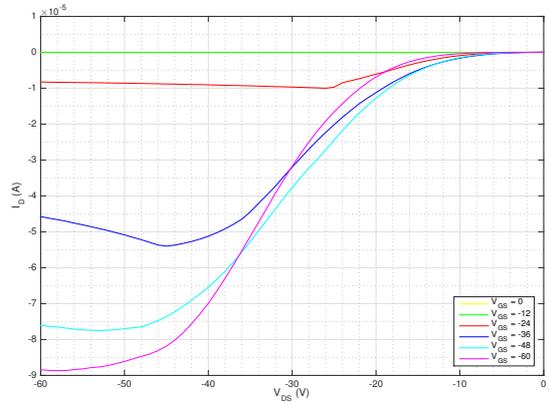


Figure 2. Output from 04/20/2016. The curves differing from an ideal output is due to the current crowding effect.

V. IMPROVEMENTS AND FURTHER STUDY OF THE OTFT

One possible way to improve the performance of the OTFT would be to reduce the negative impact of the crowding effect. Consequently, it would be desirable to introduce a hole transport layer between the semiconductor and the contacts to collect the holes more efficiently, which experimentally has been found to reduce the crowding effect. The reason why it works is not completely defined: in some cases it modifies the structure at a molecular level, and in other cases it is unknown. One candidate material to use could be MoO₃.

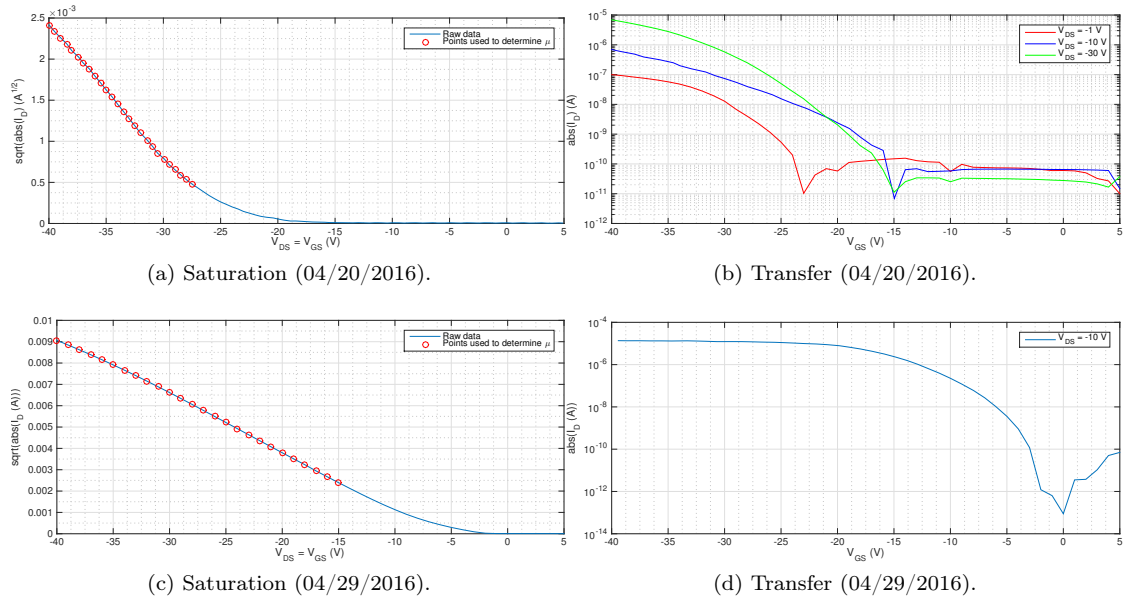


Figure 3. Characteristic curves obtained in the indicated dates. Transistor was fabricated on 04/20/2016.

The stability of organic transistors is not only determined by the evolution of the materials with time, but also by the shift experienced in the threshold voltage when a bias is applied to the gate electrode, the so-called stressing [9]. This is caused by trapped charge carriers at the semiconductor-insulator interface. Consequently, higher gate voltages have to be used. Therefore, an interesting study would be to analyze the outputs of the OTFT after stressing it, for example, for 0 min, 10 min, 30 min, 90 min, and 180 min. However, this study was not carried out for strategic decisions within the project.

VI. CONCLUSIONS

We remind that our goal was to reproduce, in the possible ways, the OTFT presented in [1]. The mobility, though being enough good, was one order of magnitude below the desired. With respect to the threshold voltage, the evolution of it due to the oxygen exposure

is quite interesting. However, an exhaustive study of the evolution of the threshold voltage within more time should be performed to determine the degree of stability. The current ratio I_{on}/I_{off} was found to be lower, but it remains approximately to the desired order of magnitude.

We conclude that the compound BOBTP presents good performance parameters to be used as the semiconductor layer of a thin-film transistor. Still, we think that using a polystyrene SAM instead of an octadecyltrichlorosilane (OTS) SAM is the reason why our results differ from the results in [1].

ACKNOWLEDGMENTS

We wish to acknowledge Dr. Joaquim Puigdollers for his guidance and for explaining to us all the details in the fabrication and function of organic TFTs. In addition, we would like to thank Marta Reig for her assistance in the laboratory.

[1] H. Cho, S. Lee, N. S. Cho, G. E. Jabbour, J. Kwak, D.-H. Hwang, and C. Lee, ACS ap-

plied materials & interfaces **5**, 3855 (2013).

- [2] C. Reese, M. Roberts, M.-m. Ling, and Z. Bao, *Materials today* **7**, 20 (2004).
- [3] O. D. Jurchescu, J. Baas, and T. Palstra, arXiv preprint cond-mat/0404130 (2004).
- [4] S. Ahmad, *Journal of Polymer Engineering* **34**, 279 (2014).
- [5] H. Zhang, Y. Wang, K. Shao, Y. Liu, S. Chen, W. Qiu, X. Sun, T. Qi, Y. Ma, G. Yu, *et al.*, *Chemical communications*, 755 (2006).
- [6] Y. Wang, H. Wang, Y. Liu, C.-a. Di, Y. Sun, W. Wu, G. Yu, D. Zhang, and D. Zhu, *Journal of the American Chemical Society* **128**, 13058 (2006).
- [7] U. Farok, Y. Falinie, A. Alias, B. Gosh, I. Saad, A. Mukifza, and K. Anuar, in *Artificial Intelligence, Modelling and Simulation (AIMS), 2013 1st International Conference on* (IEEE, 2013) pp. 459–461.
- [8] A. Benor, A. Hoppe, V. Wagner, and D. Knipp, *Organic Electronics* **8**, 749 (2007).
- [9] H. Gomes, P. Stallinga, F. Dinelli, M. Murgia, F. Biscarini, D. De Leeuw, T. Muck, J. Geurts, L. Molenkamp, and V. Wagner, *Applied Physics Letters* **84**, 3184 (2004).